THEORETICAL & APPLIED MECHANICS LETTERS **3**, 021005 (2013)

Distinct element method investigation on mechanical behavior within shear bands in granulates under the Earth and the Moon conditions

Mingjing Jiang,[a)] and Wangcheng Zhang

Department of Geotechnical Engineering, Key Laboratory of Geotechnical and Underground Engineering of Ministry of Education, Tongji University, Shanghai 200092, China

(Received 6 December 2012; accepted 17 January 2013; published online 10 March 2013)

Abstract This letter mainly aims to investigate the mechanical behavior within shear bands in regolith both under the Earth and the Moon conditions via the distinct element method, in which a novel contact model considering interparticle van der Waals forces and rolling resistance is employed. The results show that for regolith under both conditions the stress paths are almost identical inside and outside the shear bands but void ratio, average pure rotation rate, and strain paths are rather distinct with dilation, particle rotation and the second invariant of strain tensor mainly occurring within the bands. However, the regolith under the Moon condition has higher peak strength and more significant strain localization than those under the Earth condition. © *2013 The Chinese Society of Theoretical and Applied Mechanics.* [doi:10.1063/2.1302105]

Keywords lunar regolith, shear band, van der Waals forces, micromechanics, distinct element method

The exploration of the Moon space is of crucial importance for future human activities and has aroused the interest of great nations all over the world. For practical engineering on the Moon, the knowledge of mechanical behavior of regolith covered on the lunar surface is in essence required. It has been accepted that the lunar regolith is a kind of cohesive granulates rather than cohesionless dry sands, which is closely related to the microscopic features of lunar regolith and the special environmental conditions on the Moon.[1,2]

The formation of shear band in granulates affects many aspects of mechanical behaviors, e.g., strain softening, volumetric dilation and energy dissipation. For granulates under the Earth condition, shear band has been thoroughly studied through laboratory experiments and numerical simulations.[3–5] However, the mechanical behaviors of regolith on the Moon, particularly within the shear band remain unknown, which gives the motivation of this paper. The distinct element method (DEM) originally developed by Cundall and Strack[6] has emerged as a powerful tool for investigating the mechanical behavior macroscopically and microscopically.[7,8] Some DEM simulations for the lunar regolith have been reported,[9,10] however, no robust contact laws for lunar regolith have been proposed to simultaneously consider grain shape, crushability and short-range forces.

Therefore, this paper aims to conduct a DEM investigation on the behavior within shear bands for regolith under the Moon and the Earth conditions. A novel contact model incorporating interparticle van der Waals forces (WF) and rolling resistance is employed. The void ratio, average pure rotation (APR) rate, and stress and strain paths within shear bands are analyzed.

The novel contact model takes into account WF which is induced by the dipole–dipole potential energy between two neighboring molecules and particles can be calculated as follows[2]

$$F_{\mathrm{v}} = \frac{Aa^2}{6D^3} + \frac{Ar}{12D^2}, \tag{1}$$

where A is the Hamaker coefficient taken as 4.3×10^{-20} J for lunar regolith, a is the radius of contact area, r is the common radius, and D is the absorbed gas thickness. Mainly owing to the ultra-high vacuum in the lunar surface, the value of D is much lower than that in the Earth surface. Consequently, the WF for regolith under the Moon condition are rather significant, however on the Earth it turns relative weak compared to the gravitational forces.[1,11] It also should be noted that other inter-molecule forces such as electrostatic forces and static-image charge forces are not considered in current paper.

The contact model includes WF in three components, i.e. the normal, tangential and rolling contact models, as shown in Fig. 1. The contact law for each component is characterized by the constant stiffness and the threshold distinguishing the linear elastic and plastic stages. Due to the WF effect, the normal unbalanced force at the area-contact for either of the two discs, F_{n}, is expressed by

$$F_{\mathrm{n}} = K_{\mathrm{n}}u - F_{\mathrm{v}}, \tag{2}$$

where K_{n} is the normal contact stiffness (N/m) and u is the normal overlap between two discs. The sliding resistance in tangential component and the rolling resistance in rolling component are both controlled by the Mohr–Coulomb criterion, involving in two components from load and the WF. Particularly in the rolling component, the contact couple M can be described as follows

$$M = K_{\mathrm{m}}\theta_{\mathrm{r}}, \quad \theta_{\mathrm{r}} \leqslant \theta_{\mathrm{r}}^0, \tag{3a}$$

$$M = \frac{1}{6}(F_{\mathrm{n}} + F_{\mathrm{v}})B, \quad \theta_{\mathrm{r}} > \theta_{\mathrm{r}}^0, \tag{3b}$$

[a)]Corresponding author. Email: mingjing.jiang@tongji.edu.cn.

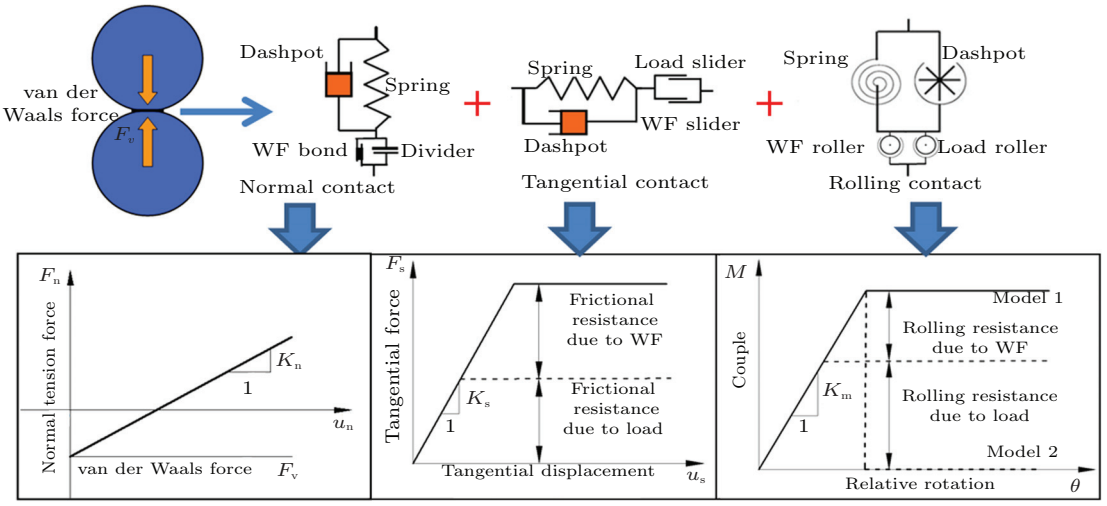

Fig. 1. Contact model for lunar regolith in normal, tangential and rolling directions.

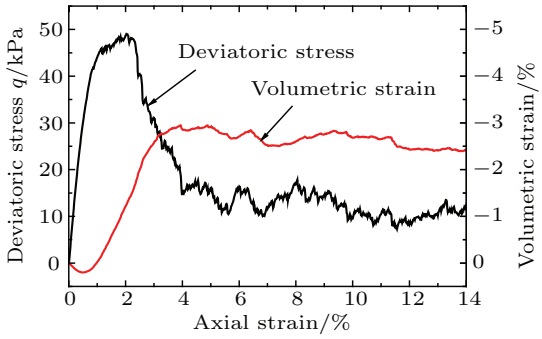

(a) For regolith under Earth condition

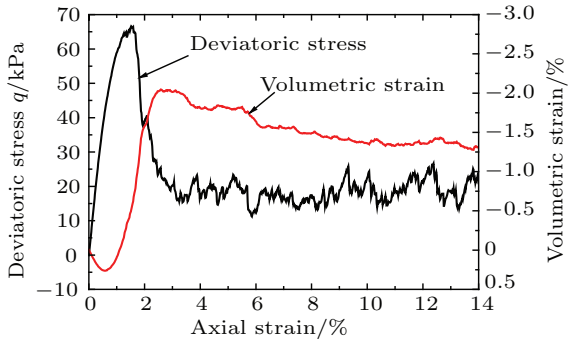

(b) For regolith under Moon condition

Fig. 2. Global stress–strain response and volumetric behavior.

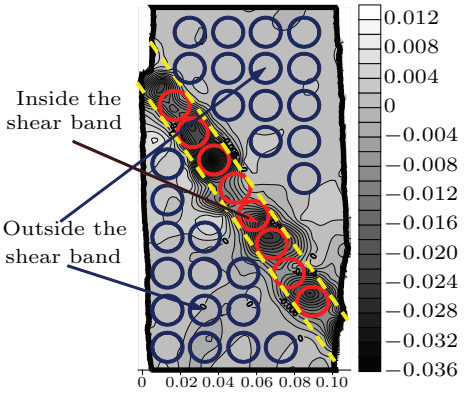

(a) For regolith under Earth condition

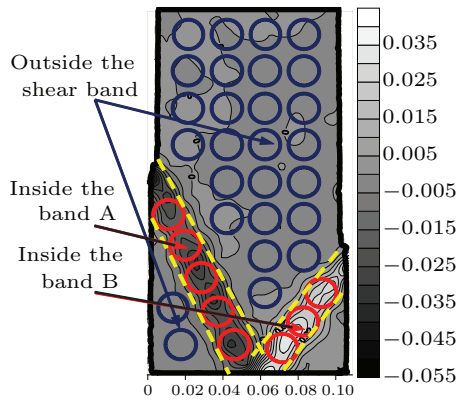

(b) For regolith under Moon condition

Fig. 3. Spatial distributions of average pure rotation rate and measurement circles at axial strain of 6%.

where θ_r is the relative particle rotation, K_m ($K_m = K_n B^2/12$) is the rolling stiffness, B is the width of contact area, $B = \beta r = 2a$, with β denoting the shape parameter), and $\theta_r^0 = 2(F_n + F_v)/(K_n B)$ is the threshold rotation angle. The contact model without WF effect comes from Refs. 7, 12.

The initial sample has a dimension of 1 078 mm (weight) × 2 154 mm (height) and is composed totally of 24 000 particles. These particles are prepared at an initial planar void ratio of 0.22, generating a medium dense sample. The DEM granulate is characterized with its size ranging from 0.5 mm to 2 mm, its mean diameter d_{50} as 1.3 mm and uniformity coefficient C_u (i.e., $C_u = d_{60}/d_{10}$) as 2.35. The normal and tangential contact stiffness takes the value of 7.5×10^7 N/m

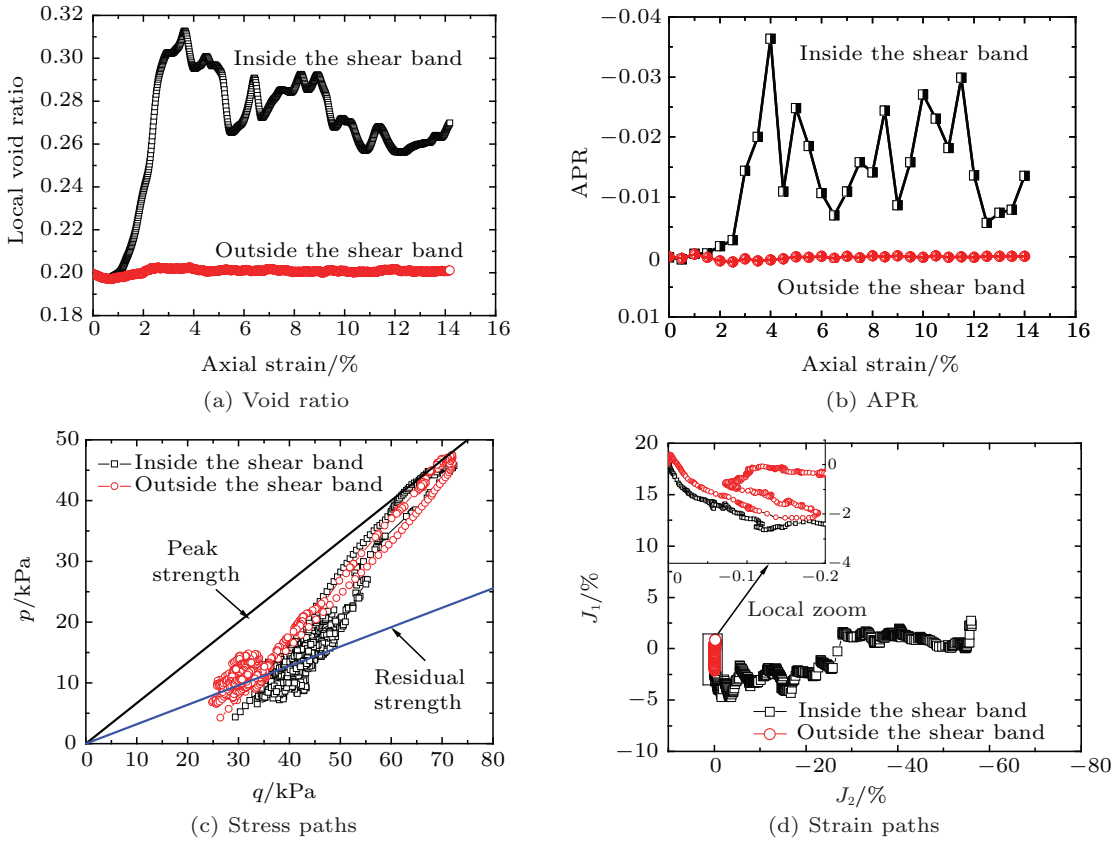

Fig. 4. Behaviors within shear band for regolith under the Earth conditions.

and 5×10^7 N/m, respectively. The interparticle friction coefficient is equal to 1.0 while the wall-particle contact is assumed to be frictionless. The density of the particle is 3 100 kg/m^3 and the shape parameter β is 1.3. Noting the high value of the interparticle friction coefficient and shape parameter is used to reflect the relative high value of frictional angle for regolith under the Moon condition. In addition, the absorbed gas thickness for regolith under the Moon condition is set to 1.5×10^{-9} m and WF is neglected for regolith under the Earth condition.

The multilayer under-compaction method[13] was used to generate the initially homogenous samples. Then, it was subjected to an isotropic confining pressure (25 kPa in this study) until the system achieved equilibrium. Finally, the sample was compressed vertically at a constant strain rate of 0.5% per minute while the pressure remains constant on the lateral flexible boundaries which were employed to facilitate the full development of shear bands.

Figure 2 presents the global relationships of deviatoric stress and volumetric strain against axial strain both for regolith under the Earth and the Moon conditions. The deviatoric stress is defined as $q = (\sigma_1 - \sigma_3)/2$. Figure 2 shows that the regolith under the Moon condition has higher peak and residual strengths than those under the Earth condition. Figure 3 provides the spatial distributions of averaged pure rotation rate (APR) and the measurement circles at axial strain of 6% both for regolith under the Earth and the Moon conditions. The APR links the particle rotation with the energy dissipation and is considered as positive in the counterclockwise direction.[14,15] Figure 3 shows that the APR is significantly localized within shear bands but in different patterns in two cases. The Moon condition leads to two shear bands (the left and the right one marked with band A and band B respectively, as shown in Fig. 3) and larger shear band inclination compared with one shear band on the Earth condition.

We shall analyze the void ratio, APR, stress and strain paths inside the shear bands in both cases. In description of the stress path, the mean effective stress p ($p = (\sigma_1 + \sigma_3)/2$) and deviatoric stress q are used. The strain path is expressed in terms of the first invariant J_1 and the second invariant J_2 of the strain tensor ε_{ij},

$$J_1 = \varepsilon_{ii}, \tag{4a}$$

$$J_2 = \varepsilon_{ii}\varepsilon_{jj} - \varepsilon_{ij}\varepsilon_{ij}. \tag{4b}$$

Note that the averaged value of the data from all the measurement circles inside or outside the shear bands is used.

Figures 4 and 5 give the behaviors within the shear bands for regolith under the Earth and the Moon conditions, respectively, which show that in the both cases: (1) The void ratio and the APR inside the shear bands

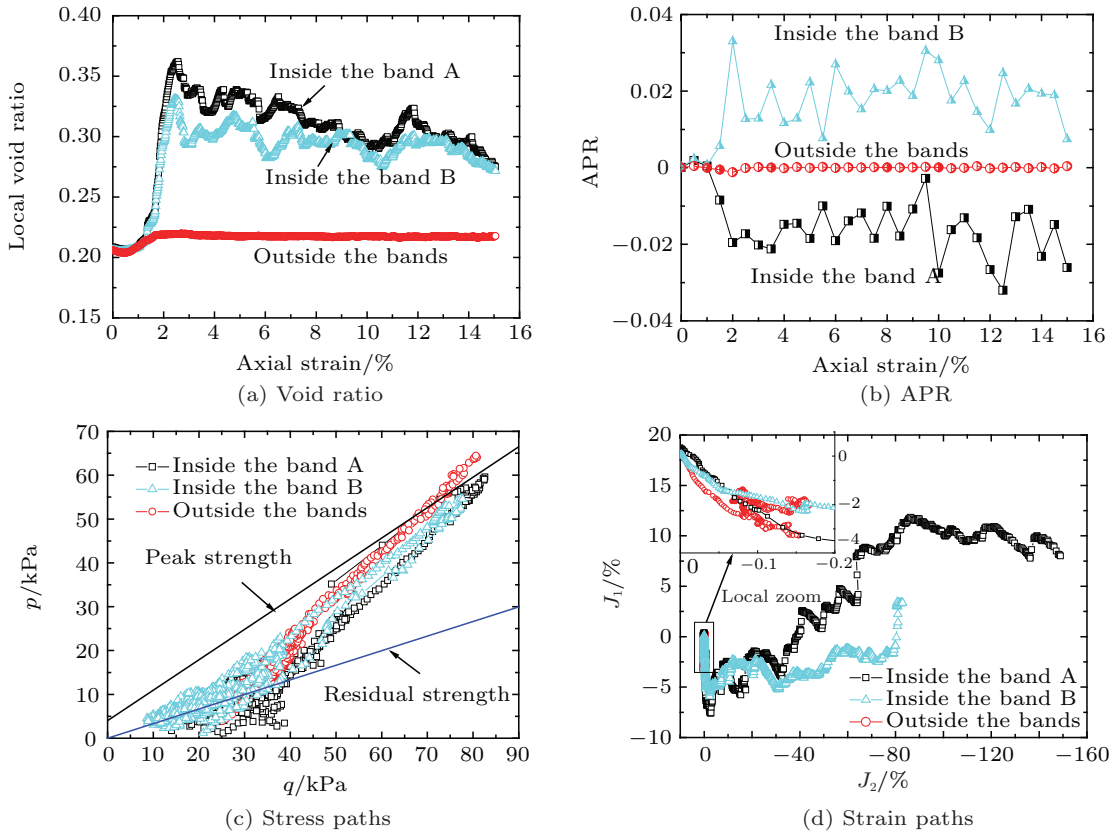

Fig. 5. Behaviors within shear bands for regolith under the Moon conditions.

are much larger than those outside the bands after the onset of strain localization, indicating that the dilation and particle rotation mainly happen within the bands; (2) The soils inside and outside the bands experience similar stress paths, i.e. firstly loading to the peak and then unloading to the residual state; (3) With the increase of axial strain, J_2 remains near zero outside the bands but continually increases inside the bands. These observations reveal that the soils yield inside the bands but remain intact outside the bands. Moreover, Figs. 4 and 5 show that under the Moon condition: (1) The regolith shows larger value of void ratio within bands, as a result of the existence of WF; and (2) The regolith exhibits greater value of J_2, than those under the Earth condition. These two findings show that the existence of WF enhances the shear band formation.

DEM was used in this paper to investigate the mechanical behavior within shear bands in granulates under both the Moon and the Earth conditions. The main conclusions are as follows.

In both cases, similar stress path is experienced all over the sample while the dilation, particle rotation and J_2 are mainly concentrated inside the shear bands. Granulates yield inside the bands while remain intact outside the bands. The regolith under the Moon condition has higher peak strength and steeper inclination of shear band compared with the regolith under the Earth condition. In addition, the dilation, particle rotation and J_2 within the shear bands are more significant in regolith under the Moon condition than those under the Earth condition, showing that WF facilitates the formation of shear band.

This work was supported by China National Funds for Distinguished Young Scientists (51025932), the National Natural Science Foundation of China (51179128), and Program of Shanghai Academic Chief Scientist (11XD1405200). In addition, the authors thank the first author's former MSc student, Min Zheng, for his carrying out DEM simulations.

1. C. S. Chang, and P. Y. Hicher, J. Aerosp. Eng. **22**, 43 (2009).
2. M. J. Jiang, L. Q. Li, and Y. G. Sun, J. Aerosp. Eng. **25**, 463 (2012).
3. J. Desrues, and G. Viggiani, Int. J. Numer. Anal. Meth. Geomech. **28**, 279 (2004).
4. M. J. Jiang, H. H. Zhu, and X. M. Li, Front. Archit. Civ. Eng. China **4**, 208 (2010).
5. M. J. Jiang, H. B. Yan, and H. H. Zhu, et al., Comput. Geotech. **38**, 14 (2011).
6. P. A. Cundall, and O. D. L. Strack, Geotechnique **29**, 47 (1979).
7. M. J. Jiang, H. S. Yu, and D. Harris, Computers and Geotechnics **32**, 340 (2005).
8. M. J. Jiang, S. Leroueil, and J. M. Konrad, Journal of Engineering Mechanics, ASCE **131**, 1209 (2005).
9. H. Nakashima, Y. Shioji, and T. Kobayashi, et al., J. Terramechanics **48**, 17 (2011).

10. H. H. Bui, T. Kobayashi, and R. Fukagawa, et al., J. Terramechanics **46**, 115 (2009).
11. H. A. Perko, J. D. Nelson, and W. Z. Sadeh, J. Geotech. Geoenviron. Eng. **127**, 371 (2001).
12. M. J. Jiang, D. Harris, and H. S. Yu, Int. J. Numer. Anal. Meth. Geomech. **30**, 723 (2006).
13. M. J. Jiang, J. M. Konrad, and S. Leroueil, Comput. Geotech. **30**, 579 (2003).
14. M. J. Jiang, D. Harris, and H. S. Yu, Int. J. Numer. Anal. Meth. Geomech. **29**, 643 (2005).
15. M. J. Jiang, H. S. Yu, and D. Harris, Mechanics Research Communication **33**, 651 (2006).